Hybrid Ultrasound MRI for Improved Cardiac Imaging and Real-Time Respiration Control

David A. Feinberg,[1–3]* Daniel Giese,[6] D. Andre Bongers,[4] Sudhir Ramanna,[1] Maxim Zaitsev,[6] Michael Markl,[6] and Matthias Günther[1,4,5]

A hybridized dual-imaging system combining real-time ultrasound imaging and MRI was utilized for cardiac imaging at 1.5 T and 3 T. The ultrasound scanner with a programmable software interface was connected via computer to the MRI scanner. Electronic noise was eliminated with electromagnetic shielding and grounding to the screen room. At 3 T, real-time prospective motion compensation in dynamic cine cardiac imaging was implemented using B-mode ultrasound imaging. The ultrasound technique avoided drawbacks such as signal saturation or steady-state interruption of the MR navigator gating. At 1.5 T, a low-latency real-time feedback to balanced steady state free precision MR imaging was performed in three normal volunteers. Results showed active tracking of the heart during respiratory motion and improvement in time-averaged cardiovascular images. Future studies can fully exploit the potential of the high-frequency position information provided by the ultrasound system for more advanced applications in real-time organ tracking. Magn Reson Med 00:000–000, 2010. © 2009 Wiley-Liss, Inc.

Key words: ultrasound; MRI; cardiac MRI; navigator echo

For cardiac MRI, several different approaches exist to overcome respiratory and cardiac motions that otherwise degrade image quality. Some of the earliest cardiac gating methods utilizing ECG triggering produced clinically useful images of the myocardium and ventricular function (1). With navigator echoes (2), direct measurement and correction of respiratory and cardiac dependent motion can be achieved in "real time" during the MR data acquisition (3–5). Retrospective correction techniques using navigator echoes have been successfully applied (6,7). Self-navigator techniques have also been utilized (8). Commonly used MR navigator gating techniques in combination with adaptive phase-encoding-line reordering schemes, however, suffer from disadvantages, including steady-state interruption, signal saturation, and low scan efficiencies (9,10). Slice-following methods have been proposed, often, however, restricted by the uncertain correlation between heart and diaphragm motion (11).

A very different approach to track cardiac position and cardiac phase is with ultrasonography or ultrasound (US) imaging, which is a well-established diagnostic imaging modality that employs a transducer to send sound waves in the megahertz range into the subjects' body. The sound waves are created in the transducer by electromechanically operating piezoelectric crystals and travel through the tissue in the form of mechanical compression/decompression waves at a speed of approximately 1540 m/sec. The subsequent detection of sound waves partially reflected back to the transducer at boundaries between structures with different mechanical compressibility permits real-time imaging at a frame rate of 100 frames per second or more. Due to their low amplitudes and high frequencies, the sound waves are normally not detectable with MRI (except for the special case of standing waves (12)) and, theoretically, the electromagnetic MR signal would not interfere with the US signal detection. Consequently, the two modalities can be operated simultaneously without one adversely affecting the other (13,14). By creating a hybrid modality, one could in principle use US imaging, US Doppler, or US M-mode positional data to obtain real-time information on cardiac motion and then to adjust the time window when the MR image is acquired or to track the heart position. This is similar to prospective navigator echoes in the MR data acquisition scheme (4–6,15).

Used for external respiratory motion tracking, US offer several advantages since information on breathing patterns can be acquired simultaneously with the MR acquisition and integrated into the imaging procedure in real time. Recently, a real-time US guidance system was proposed whereby MRI and US imaging are performed simultaneously (14). Positional information measured in two-dimensional (2D) US images can be transferred to the MRI scanner in real time to detect respiratory- and cardiac-driven changes in position of body organs. The technique has been developed and tested in motion phantoms. To date, the potential of US imaging for motion tracking has not been fully exploited due to limitations regarding hardware and software integration.

Presented here are the first in vivo evaluations of the hybrid US-MRI guidance system. Human cardiac imaging

[1]Advanced MRI Technologies, Sebastopol, California, USA

[2]Department of Radiology, University of California, San Francisco, California, USA

[3]Institute of Neuroscience, University of California, Berkeley, California, USA

[4]Mediri GmbH, Heidelberg, Germany

[5]Department of Neurology, Klinikum Mannheim, University Heidelberg, Germany

[6]Department of Diagnostic Radiology, Medical Physics University Hospital Freiburg, Germany

*Correspondence to: David A. Feinberg, Advanced MRI Technologies, 652 Petaluma Ave., Suite J, Sebastopol, CA 95472.
E-mail: david.feinberg@advancedmri.com

is demonstrated first with US respiratory gating. As a second demonstration of feasibility, US is used as a short-latency real-time feedback for prospective respiratory motion correction in balanced steady state free precision (SSFP) cardiac and vascular imaging.

MATERIALS AND METHODS

All experiments were performed on 1.5-T (Sonata; Siemens, Germany) and 3-T (Trio; Siemens, Erlangen, Germany) MR scanners with standard gradient systems (40 mT/m maximum, 200 mT/msec/m slew rate). The studies were performed on three normal volunteers at 1.5 T and one volunteer at 3 T. All human studies were performed after informed consent and with institutional review board approval.

Experimental Setup

The system designed for US tracking in an MR scanner consists of four major components:

1. Standard clinical digital 2D US imaging device, including a cardiac transducer (3.5 MHz)
2. US transducer/probe mounting device
3. A personal computer (PC) used to receive the US data and perform motion tracking
4. Clinical 1.5-T and 3-T MR systems with sequence development environment installed

The experimental setup of the US-MR system is illustrated in Fig. 1.

US Device

The US scanner (Echo Blaster 128; Telemed) is compact and has a programmable software interface. The US device is placed in close proximity to the MR and connected to a PC outside of the scanner room through a 15-foot-long USB cable. To prevent noise at the radiofrequency detection range of the MR scanner, electromagnetic shielding of both the US system and transducer was necessary. Shielding was achieved by placing the aluminum foil around the US beam former probe and cables.

At 1.5 T, the US transducer window was covered with metal-coated Mylar. The coated Mylar plastic is thin enough permit the passage of US pulses yet thick enough to shield the electromagnetic radiofrequency radiation at frequencies that can be detected by the MR receiver coil. All system components, including the US device, transducer, and cables, were grounded to the magnet screen room shielding by placing the device on aluminum foil in contact with the screen room floor and by using 1-inch-wide, 32-gauge, tinned, ground braid cable.

At 3 T, the US beam former and its battery were placed in a self-built copper cage. For both 1.5 T and 3 T, the PC was placed outside of the magnet room in the MR control room. The computer was connected to the US device by means of the USB cable passed through a waveguide filter in the radiofrequency shielding.

Mounting Device

For both 1.5- and 3-T setups, a mounting system to hold the US transducer on the subject, while they are on the MR table, was machined from nonmagnetic material of rigid fiberglass and aluminum brackets to be compatible with the magnetic field environment. The halo-shaped mounting system is readily attached to or removed from the patient table with brass hooks. The rigidity of the mounting system and the adjustable articulated arm holds the US at a constant position (see also Fig. 1). The desired US views were first determined by the technologist before the US probe/transducer was clamped to the mounting device to hold the position against the body.

Tracking Algorithm

A motion-tracking algorithm using real-time US data was implemented based on contour-tracking algorithms useful in statistically noisy data, described elsewhere (12–16). The CONDENSATION algorithm samples the state space numerous times in a random manner but follows a deterministic diffusion equation, which describes the possible movement of the structure. State space was restricted to affine transformations only.

The US interface uses Microsoft DirectX technology that is component object model based. We also use Microsoft Foundation Class to implement the necessary graphic user interface. The tracking algorithm using the implementation of the condensation process (15) is operational at standard noise levels in the US images. Improvements included the definition of weights for each sample during the condensation process. The computer software algorithm sampled the US raw data obtained in real time. The entire computation time of the tracking algorithm is less than 1 ms. The data of the calculated positional information were sent to the MR system via a TCP/IP connection using named pipes.

The US device had its driver software installed on the PC to enable the use of a single PC to run both the US scanner and the tracking software. The removal of the PC from the scanner room not only reduced noise but also had a practical advantage of permitting real-time graphic overlay display of the tracked regions on the dynamic US images. The tracking software was implemented in C++ on a Windows XP computer with a clock speed of 2.8 GHz and 2048 Mbyte random access memory.

We devised the simplest system to register the orientation of the US probe with respect to the coordinates of the MR system, using a protractor to measure within a degree the angle of the probe. The angular measurement was made using the horizontal and vertical laser positioning system that is a part of the MR scanner. The motion tracking was performed on only one axis, in the cranial-caudal (head-foot) direction. Extension of the tracking algorithm to incorporate two spatial axes, using the 2D US images, or in three-dimensional utilizing two or more probes, is certainly possible but beyond the scope of this work.

Hybrid US MRI Respiration-Gated GRE CINE Imaging

The implemented GRE pulse sequence was based on a segmented *k*-space, radiofrequency-spoiled, time-resolved (CINE) 2D GRE sequence with prospective ECG
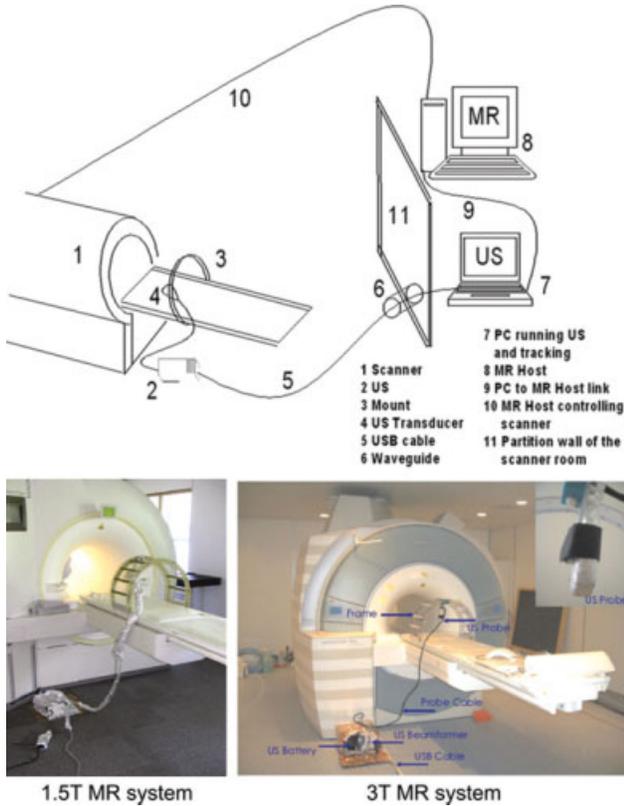
FIG. 1. Top: Diagram shows system and network of computers between MRI scanners and US. Bottom: Fiberglass mounting system holding US transducer in position on the patient bed of the MR scanner at 1.5 T (left) and 3 T (right).

time frames; and 2-fold acceleration ($2\times$) using GRAPPA. In vivo data of ventricular motion in the short axis plane were acquired with spatial resolution of $1.4 \times 1.4 \times 8$ mm^3.

Scan-Plane Dynamic Updating

The scan planes for all slices are predefined by the pulse sequence parameters, as well as the selected FOV, and usually remain fixed. However, to track a moving object in all three dimensions, the individual slice locations are moved in between steps in the phase-encoding table. Therefore, instead of being static, the scan planes were updated dynamically based on the heart position as determined by the continuous US scan.

The tracking algorithm detected the position of the moving structure or diaphragm and the US coordinates were transformed to the corresponding coordinates of the MR scanner, and this information was sent to the MR scanner control computer, where it affected the running pulse sequence.

Hybrid US MRI Balanced SSFP Imaging

Cardiac imaging was performed using a balanced SSFP pulse sequence (16). The sequence automatically used the shortest possible repetition time for a given parameter set (FOV, sampling bandwidth, matrix size). The current slice position and orientation were read from a set of variables, which was updated as soon as new positional data from the US system were available. The sequence then calculated the necessary gradient and radiofrequency-pulse commands and sent the information to the MR control system. Ideally, the control information of a single line should be processed immediately to provide the shortest latency time (delay time) to take advantage of the most recent position information available from the US. However, the MR pulse sequence has to run continuously; therefore, instruction sets for multiple MR signals (multiple pulse repetition times in the balanced SSFP sequence) instead of one pulse repetition time has to be sent to the MR control system in a block. Usually 20 ms were sufficient to ensure that there was always instruction code in the queue. For a typical repetition time, instruction code for eight pulse repetition time had to be grouped; therefore, the US information is currently limited in its effect on the MR data acquisition to 20-ms intervals between updates. The balanced SSFP image and sequence had the parameters echo time = 1.43 ms, bandwidth = 1502 Hz/pixel, pulse repetition time = 2.85 ms, matrix size = 128×128, FOV = 300×300 mm.

RESULTS

US Shielding

One challenge in the US guidance system was to adequately reduce electronic noise from the US scanner introduced into the MR images. In addition to shielding of the US transducer, all cables and the US scanner adjacent to the magnet, the direct grounding of the US scanner to the MR screen room floor was critical to achieve noise reduction. At 1.5 T, measurements of signal were

gating. For respiration control, US information was used similarly to often-used (9) MR navigator sequence. B-mode US images of the diaphragm were acquired simultaneously with the MR data, whereas the US probe was positioned below the diaphragm and the beam was directed superiorly, critical for respiratory tracking. This subdiaphragm window and other standard US windows to visualize the heart are possible, depending on the radiofrequency coil position and geometric design. The tracked position of the diaphragm was used to monitor respiration and to decide whether to accept or reacquire the MR data (2) in real time. The decision was taken at end diastole of every ECG cycle: If falling inside a predefined acceptance window, the data were accepted; if not, the data were reacquired during the next ECG cycle. In order to reduce ghosting artifacts, respiratory gating was combined with an adaptive line-reordering algorithm (9,10) and the acceptance window position was dynamically adjusted during measurement.

Preliminary image comparison was made with acquired MR navigator-gated images using a simple cross-pair MR navigator instead of the US signal at the end of every ECG cycle. The GRE sequence had the following parameters: field of view (FOV), 308×380 mm^2; matrix size, 168×256; slice thickness, 8 mm; flip angle, $15°$; number of cardiac time frames, 24; pulse repetition time, 3.7 ms; echo time: 1.33 ms; temporal resolution, 32 ms (6 *k*-space lines per ECG cycle per time frame); 40
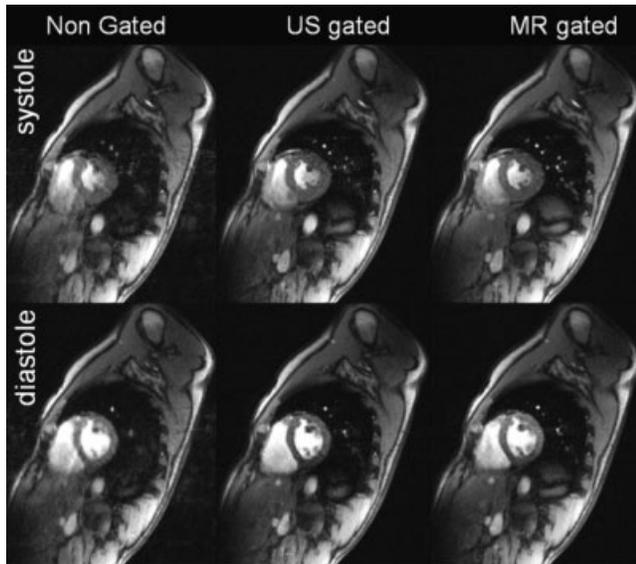
FIG. 2. The nongated free-breathing short-axis views (acceptance rate 100%) show substantial motion artifacts throughout the ECG cycle. Acquired US-gated short-axis views with identical sequence parameters and a data acceptance rate of 29% show clearly reduced ghosting and blurring due to motion and demonstrate similar image quality to MR navigator-gated acquisitions (acceptance rate 32%).

made in the main pulmonary artery and noise in air adjacent to the right abdominal wall, (signal, noise), (211, 5.3) SNR = 39.8, respectively, with US system turned off, and (228.1, 6.0), SNR = 38.0, with the US tracking system enabled. This small increase in noise in utilizing US guidance is much smaller than when there was incomplete grounding in the human imaging scan, not shown, (252.4, 24.1) SNR = 10.47, with the US tracking system enabled. Similar shielding effects were achieved at 3 T, whereas residual noise was reduced by more completely shielding the US system.

Structure Tracking in US Images

The tracking algorithm provided fast and robust tracking of the targeted structure at most times. Problems occurred when the target structure moved out the FOV. However, the tracking algorithm was able to repeatedly find the structure as soon as it reappeared within the FOV.

In Vivo US/MR Respiration-Gated GRE CINE Imaging

Compared to ungated images, the use of US as a navigator signal in GRE imaging considerably improved blurring and ghosting due to subject respiration throughout the ECG cycle (as shown in Fig. 2). First acquisitions demonstrate the feasibility of US-gated cardiac CINE imaging at 3 T during free breathing. A detailed comparison between the presented US gating and the MR navigator gating is of interest but beyond the scope of this work. Figure 2, however, shows similar image quality between US gating and MR navigator gating (with similar acceptance rates) and shows no visible artifacts from the US device.

Hybrid US MRI Balanced SSFP Imaging

At 1.5 T, the US tracking of respiratory motion directly reduced the displacements of the heart in cine SSFP imaging, Fig. 3. Figure 3b shows a column of pixels (M-mode image) obtained from each of the cine images, placed on the horizontal axis showing relative timing in the cine-acquisition. A reduction of relative vertical displacement of the heart is seen when using US guidance as compared to without and yet is not at constant position as during breath holding. Further unlike breath-hold acquisition, the US navigation expectedly increases the displacements of the noncorrelated higher mediastinum structures as the resulting coordinate transformation to the moving reference frame of the heart transfers the periodic displacements to the relatively stationary structures, including the great vessels and superior mediastinum (viewed in the upper tracing of the MR M-mode). Figure 3c shows the similar comparison with ECG gating enabled with US navigation. There is reduced variation caused by respiratory displacement and by varying cardiac phase when both systems are enabled.

Imaging results were obtained utilizing true FISP (SSFP) images in coronal orientation covering the thoracic cardiovascular system. Figure 4 shows a comparison of signal averaging utilizing the cine-SSFP images with and without US navigation. There were 40 image frames averaged during normal respiratory motion with ECG cardiac triggering enabled. Cardiac structures had much less blurring, and there was improved delineation of the left anterior descending artery when US navigation was enabled.

DISCUSSION

One major advantage of US tracking over MR navigator techniques is that the pulse sequence is not interrupted by competing acquisitions of navigator echoes or other k-space signals. The SSFP sequence moved to new acquisition locations without interrupting the sequence, using new position updates every eight echoes in an echo train of 128 echoes to make each image. In effect, the SSFP sequence maintained steady state while changing the slice position within and during the SSFP imaging of the heart. Such inner-sequence change in parameters is not possible to perform with MR navigator echo sequences because the time of acquiring a navigator echo within the SSFP sequence disturbs the steady-state conditions.

US tracking resulted in a transformation of the spatial reference frame, imposing relative motion on otherwise stationary structures while removing motion from the targeted heart. Thus, image quality of heart and vessels improves, while conversely, the more stationary structures, great vessels and chest wall, have increased artifact load and blurring. Several different sources of artifacts can occur in the nontracked stationary structures. When the scan plane is moved (translated or rotated, in or out of slice) during the acquisition of an image, nonmagnetized spins may move into the slice and will exhibit balanced SSFP transient behaviors since they are not in steady state. This may be more of an issue if the scan plane is tilted due to "angular amplification" of the
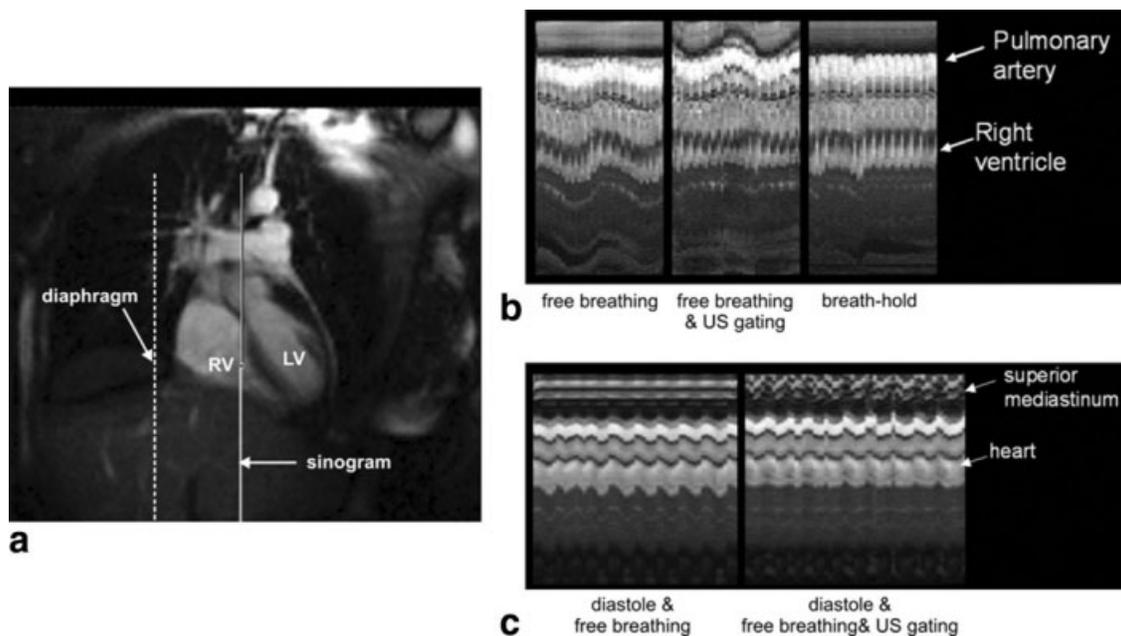
FIG. 3. **a:** SSFP image shows position of MR M-mode in heart (solid line) and position of US tracking on the diaphragm (broken line). **b:** MR M-mode of heart with (left) US tracking turned off during breathing, (middle) US tracking turned on during breathing, and (right) breath holding with a short gasp and US tracking turned off. With US tracking, there is less vertical displacement of the heart but the transformation of coordinates during MR scanning leads to increased apparent motion of the superior mediastinal structures. The breath holding eliminates both cardiac and apparent mediastinal motion. **c:** B-mode MRI of heart with ECG gating to diastolic cardiac phase; (left) without enabling US system, respiratory motion is present in heart MR M-mode; (right) with ECG gating and US tracking enabled, the cardiac displacements are markedly reduced (LV = left ventricle, RV = right ventricle).

distance. A second problem may occur when parts of the tracked slice may move into a different part of the receiver coil, where there is a change in the coil sensitivity/phase, which could be source of artifacts.

Experiments at 3 T confirmed the feasibility of a hybrid US/MR system including a real-time US feedback system. First, in vivo applications using US gating for ECG-triggered GRE CINE MRI were performed. Short-axis images showed promising results, correcting for breathing-motion effects without noticeable artifacts arising from the US device. Advantages compared to MR navigators include the absence of signal saturation and thus the possibility to directly track the heart movement in future studies.

At 1.5 T, since US tracking was positioned on the right diaphragm but not directly on the heart wall, there is small residual displacement of the heart on the vertical axis. This should likely be improved upon by tracking directly on the heart epicardium. The MR M-mode images demonstrate that when the US gating is on, there is decreased motion in the heart but greater displacement in the great vessels and mediastinum. This shows a regional correction of motion achieved with the US tracking. Similar to navigator echo-based three-dimensional coronary MRA, it may not be possible to correct for motion simultaneously in all regions of the heart due to their different directions of motion. Variations in body habitus may affect the choice of US windows to visualize the heart and choice of regions to track such as the epicardial fat.

The current work is a proof of principle that US tracking can achieve respiratory motion correction in 2D SSFP cardiac imaging and therefore might be used for the same purposes as MR navigator echoes in cardiac MRI and three-dimensional coronary MRA. Although we have demonstrated that the entire respiratory cycle can be tracked without loss in signal, there are many refinements and improvements to the US-MRI system needed to achieve its full clinical utility. One possible improvement is an external optical system for detecting the position of the US probe utilizing LEDs attached to an articulated arm mount. This would allow the optical tracking of a freely moving US transducer. Future refinement to achieve 2D to three-dimensional tracking should be possible utilizing two or more transducer probes with their image planes oriented on orthogonal axes across the heart. In addition to cardiac imaging, the hybrid US-MRI system may be used to improve imaging of abdominal organs, correcting for respiration in high field MRI, and for fetal MRI. The various configurations and applications of the US-MRI system can also be combined with existing MR navigator echo applications (17–19) to offer new approaches to improve efficiencies during data acquisition, currently limiting cardiac and coronary imaging.

Self-gating techniques represent a promising alternative to the hybrid US-MR imaging approach presented here. In recent years, several techniques have been presented to measure cardiac motion and/or respiration utilizing image-based analysis or signal changes in
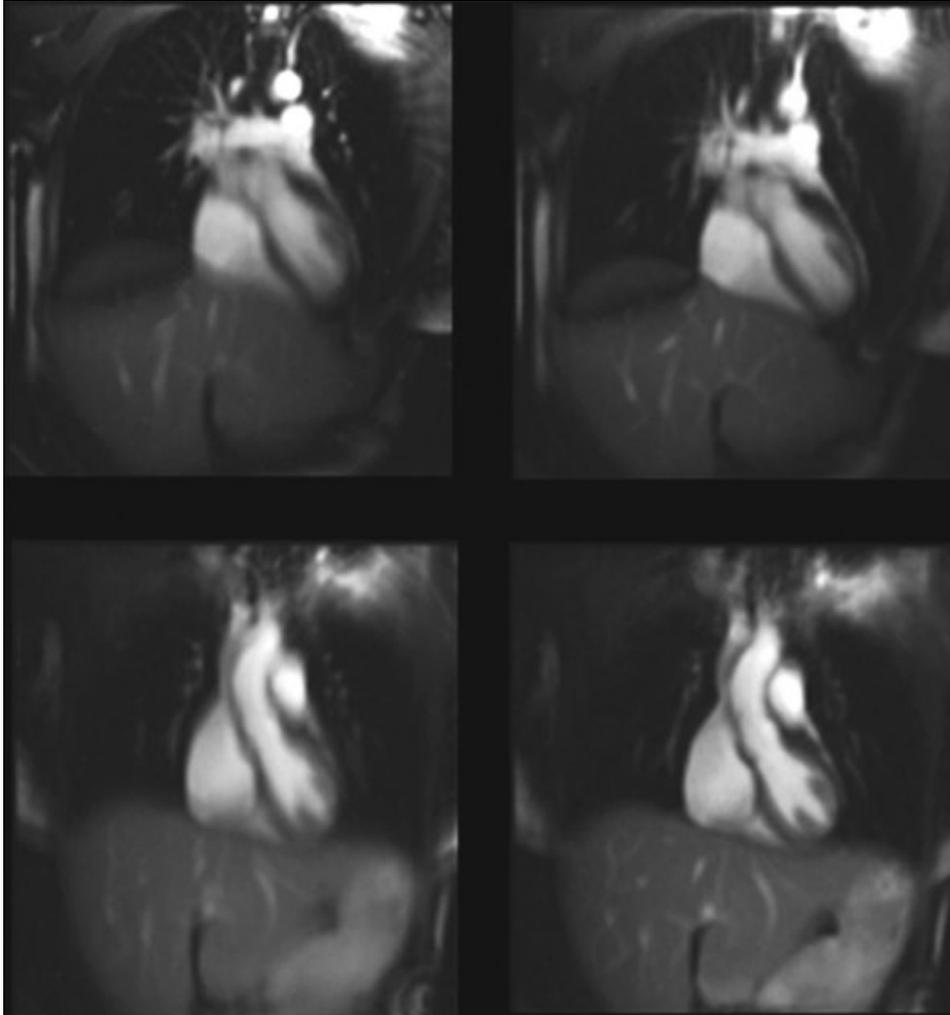
FIG. 4. Coronal images of heart (left) without and (right) with US guidance. With US guidance enabled, there is better delineation of the left anterior descending coronary artery and less blurring of the ventricular septum, inferior heart wall, and the hepatic vessels.

successively acquired *k*-space lines. Radial *k*-space sampling in combination with the evaluation of echo peak magnitude, kymogram, or 2D correlation was employed to perform cardiac triggering and respiratory gating (20,21). Other strategies used additionally acquired short navigator echoes to provide information on cardiac and respiratory motion (22,23). As a clear advantage of these techniques, no additional electrodes, respiration belts, or, as in this study, US probes are needed, resulting in reduced setup times and easy-to-perform patient examinations. However, navigator signals and image contrast used for gating can be affected by susceptibility and other sources of artifact that may affect the derived cardiac or respiration curves. In this context, US gating offers the advantage of directly mentoring the organ of interest in real time without interrupting or disturbing the simultaneous MR acquisition.

It has to be noted that the possibility to have access to US data throughout the ECG cycle, independent of the MR data acquisition, was not fully exploited for the dynamic CINE imaging used in this study. In principle, the accept/reject decision can be made at any instant of the ECG cycle. Accessing the respiration position several times during the ECG cycle and using an adequate data reordering scheme may thus help to considerably improve image quality and scan efficiency. A combination with a prospective slice-following method, including translation, rotation, and scaling parameters from the tracking algorithm, may further improve image quantity.

CONCLUSIONS

A hybrid US-MRI system was developed and utilized to image the heart during free breathing while performing an SSFP image acquisition at 1.5 T and GRE acquisition at 3 T. This new system could potentially improve cardiac MRI and permit more reliable cardiovascular imaging. One immediate application is to facilitate the lengthening of data acquisition windows during free breathing. It is also recognized that hybrid US-MRI could be used for motion correction in many different organs or for fusion of anatomic, hemodynamic, and perfusion images or for image-guided biopsies.

REFERENCES

1. Crooks LE, Barker B, Chang H, Feinberg DA, Hoenninger JC, Watts JC, Arakawa M, Kaufman L, Sheldon PE, Botvinick E. Magnetic resonance imaging strategies for heart studies. Radiology 1984;153: 459–465.
2. Ehman RL, Felmlee JP. Adaptive technique for high-definition MR imaging of moving structures. Radiology 1989;173:255–263.

3. Oshinski JN, Hofland L, Mukundan S Jr, Dixon WT, Parks WJ, Pettigrew RI. Two-dimensional coronary MR angiography without breath holding. Radiology 1996;201:737–743.

4. Danias PG, McConnell MV, Khasgiwala VC, Chuang ML, Edelman RR, Manning WJ. Prospective navigator correction of image position for coronary MR angiography. Radiology 1997;203:733–736.

5. McConnell MV, Khasgiwala VC, Savord BJ, Chen MH, Chuang ML, Edelman RR, Manning WJ. Prospective adaptive navigator correction for breath-hold MR coronary angiography. Magn Reson Med 1997;37:148–152.

6. Li D, Kaushikkar S, Haacke EM, Woodard PK, Dhawale PJ, Kroeker RM, Laub G, Kuginuki Y, Gutierrez FR. Coronary arteries: three-dimensional MR imaging with retrospective respiratory gating. Radiology 1996;201:857–863.

7. Bohning DE, Carter B, Liu SS, Pohost GM. PC-based system for retrospective cardiac and respiratory gating of NMR data. Magn Reson Med 1990;16:303–316.

8. Manke D, Nehrke K, Bornert P. Novel prospective respiratory motion correction approach for free-breathing coronary MR angiography using a patient-adapted affine motion model. Magn Reson Med 2003;50:122–131.

9. Bailes DR, Gilderdale DJ, Bydder GM, Collins AG, Firmin DN. Respiratory ordered phase encoding (ROPE): a method for reducing respiratory motion artefacts in MR imaging. J Comput Assist Tomogr 1985;9:835–838.

10. Markl M, Harloff A, Bley TA, Zaitsev M, Jung B, Weigang E, Langer M, Hennig J, Frydrychowicz A. Time-resolved 3D MR velocity mapping at 3T: improved navigator-gated assessment of vascular anatomy and blood flow. J Magn Reson Imaging 2007;25:824–831.

11. Nehrke K, Bornert P, Manke D, Bock JC. Free-breathing cardiac MR imaging: study of implications of respiratory motion—initial results. Radiology 2001;220:810–815.

12. Wu T, Felmlee JP, Greenleaf JF, Riederer SJ, Ehman RL. MR imaging of shear waves generated by focused ultrasound. Magn Reson Med 2000;43:111–115.

13. Feinberg DA, Günther M. Simultaneous MR and ultrasound imaging: towards US-navigated MRI. In: Proc. of 11th Intern. Soc. Mag. Res. in Medicine, p 90, 2000, Glasgow, Scotland.

14. Günther M, Feinberg DA. Ultrasound-guided MRI: preliminary results using a motion phantom. Magn Reson Med 2004;52:27–32.

15. Chuang ML, Chen MH, Khasgiwala VC, McConnell MV, Edelman RR, Manning WJ. Adaptive correction of imaging plane position in segmented k-space cine cardiac MRI. J Magn Reson Imaging 1997;7:811–814.

16. Isard M, Blake A. CONDENSATION—conditional density propagation for visual tracking. Int J Comput Vision 1998;29:5–28.

17. Spuentrup E, Bornert P, Botnar RM, Groen JP, Manning WJ, Stuber M. Navigator-gated free-breathing three-dimensional balanced fast field echo (trueFISP) coronary magnetic resonance angiography. Invest Radiol 2002;37:637–642.

18. Larson AC, Simonetti OP, Li D. Coronary MRA with 3D undersampled projection reconstruction trueFISP. Magn Reson Med 2002;48:594–601.

19. Huber ME, Oelhafen ME, Kozerke S, Weber OM, Boesiger P. Single breath-hold extended free-breathing navigator-gated three-dimensional coronary MRA. J Magn Reson Imaging 2002;15:210–214.

20. Larson AC, White RD, Laub G, McVeigh ER, Li D, Simonetti OP. Self-gated cardiac cine MRI. Magn Reson Med 2004;51:93–102.

21. Hiba B, Richard N, Janier M, Croisille P. Cardiac and respiratory double self-gated cine MRI in the mouse at 7 T. Magn Reson Med 2006;55:506–513.

22. Crowe ME, Larson AC, Zhang Q, Carr J, White RD, Li D, Simonetti OP. Automated rectilinear self-gated cardiac cine imaging. Magn Reson Med 2004;52:782–788.

23. Heijman E, de Graaf W, Niessen P, Nauerth A, van Eys G, de Graaf L, Nicolay K, Strijkers GJ. Comparison between prospective and retrospective triggering for mouse cardiac MRI. NMR Biomed 2007;20:439–447.